Sustainable production of pure hexanoic acid from CO_2 using microbial electrosynthesis with in-situ product recovery

Lee, Mungyu; Jankovic, Tamara; Caparrós-Salvador, Francisco; Jourdin, Ludovic; Straathof, Adrie J.J.

DOI
10.1016/j.cej.2025.169412

Publication date
2025

Document Version
Final published version

Published in
Chemical Engineering Journal

Chemical Engineering Journal 524 (2025) 169412

Contents lists available at ScienceDirect

Chemical Engineering Journal

journal homepage: www.elsevier.com/locate/cej

Sustainable production of pure hexanoic acid from CO_2 using microbial electrosynthesis with in-situ product recovery

Mungyu Lee [a,*], Tamara Jankovic [a], Francisco Caparrós-Salvador [b], Ludovic Jourdin [a,*], Adrie J.J. Straathof [a]

[a] Department of Biotechnology, Delft University of Technology, van der Maasweg 9, 2629 HZ, Delft, the Netherlands
[b] Greencovery BV, Nieuwe Kanaal 7D, 6709 PA, Wageningen, the Netherlands

ARTICLE INFO

Keywords:
Microbial electrosynthesis
Product recovery
Carbon dioxide
Sustainable bioprocess
Hexanoic acid
Carbon negative

ABSTRACT

Carbon dioxide utilization is a key strategy for sustainable chemical production and climate change mitigation. Microbial electrosynthesis (MES) offers a promising approach to convert CO_2 into organic acids and multi-carbon compounds, but its industrial application requires improved product recovery methods. In this study, we developed an integrated MES-sorption-distillation system for the recovery of pure hexanoic acid. Adsorption experiments identified conditions for C6-selective capture from C2–C6 carboxylate mixtures typically produced from MES. Subsequent desorption using CO_2 expanded methanol enriched hexanoic acid concentration by 13-fold compared to the aqueous feed, achieving 67 % recovery in a single pass, but 100 % overall, since recirculation of unrecovered carboxylates back to the MES reactor is proposed. This recirculation will enhance chain elongation, eliminate loss of unrecovered carboxylates, and reduce the need for external pH control during MES. Distillation of the desorbed mixture led to streams of pure products and reusable solvent, without losses. Notably, 87 % of the total energy demand for product formation is attributed to the MES stage, where electrical energy is directly supplied as electrons to drive microbial production. Thus, MES with the proposed recovery method enables pure hexanoic acid production with minimal losses of materials or energy and potentially allows the system to operate in a carbon-negative manner.

1. Introduction

Carbon dioxide utilization is a key strategy in mitigating climate change and advancing sustainable industrial practices. As the demand for carbon-neutral and renewable processes grows, efforts to convert CO_2 into valuable organic compounds gain significant attention [1,2]. Among various CO_2 conversion approaches (e.g., thermochemical processes, electrochemical reduction, and photochemical methods) [3–5], microbial electrosynthesis (MES) has emerged as a promising method. MES can directly couple with renewable electricity and has the advantage of employing biocatalysts under ambient temperature and pressure. It also inherently integrates carbon capture and utilization (CCU), enabling both greenhouse gas mitigation and resource valorization [6,7]. MES convert CO_2 into organic acids and multi-carbon compounds using electrotrophic microorganisms, resulting in the production of diverse chemicals such as acetate (C2), butyrate (C4), and hexanoate (C6) [8–10]. This method not only facilitates carbon capture and utilization (CCU) but also offers a potentially sustainable route for producing chemicals [11–13].

Recent advancements in MES using open (mixed) cultures have significantly improved CO_2 conversion rate and productivity. In particular, production of hexanoic acid has reached 3.2 g L^{-1} of hexanoic acid [14]. Hexanoic acid is a valuable chemical, produced in MES (Table S1) through the chain elongation pathway [15,16], and utilized, among others, as a plasticizer, an antimicrobial agent, and an ingredient in animal feed [17,18]. However, the current commercial production of hexanoic acid is limited, as it is primarily obtained as a by-product through fractional distillation of coconut or palm kernel oil, accounting for less than 1 % of the products [19–21]. This also limits the use of hexanoic acid in larger-scale applications. Due to these constraints, alternative production methods are actively being explored. Industrial production of hexanoic acid by MES still requires further development of its performance, scalability, and product recovery [22–27]. In particular, previous recovery methods have suffered from limited selectivity

* Corresponding authors.
E-mail addresses: m.lee-4@tudelft.nl (M. Lee), l.jourdin@tudelft.nl (L. Jourdin).

https://doi.org/10.1016/j.cej.2025.169412
Received 8 July 2025; Received in revised form 13 September 2025; Accepted 7 October 2025
Available online 8 October 2025

and have not achieved hexanoic acid purity above 99 %. In this study, we focus on maximizing both the recovery (amount of obtained) and purity (composition of product) of hexanoic acid through an adsorption/desorption strategy integrated with CO_2-expanded methanol, thereby addressing a critical bottleneck for achieving economic feasibility. [19,28–30].

One recovery aspect to consider is selectivity. MES, operated under open or single-culture conditions, generates C2 (acetate) and C4 (butyrate) carboxylates alongside C6 (hexanoate). C2 and C4 carboxylates have lower economic value, and their additional separation increases processing costs [19,31]. On the other hand, if not separated, they result in waste streams requiring further treatment [19,32]. Notably, C2 and C4 serve as precursors for C6 compounds [15]; therefore, their retention and recirculation within the MES system can improve C6 production yield and reduce downstream process demands. An effective separation strategy should prioritize real-time extraction of C6 carboxylates while minimizing C2 and C4 recovery to optimize MES performance and downstream processing. Other aspects to consider are recovery yield, i.e. the percentage of hexanoic acid recovered, and the concentration factor achieved during the recovery steps [33,34]. Higher concentration factors lead to lower energy costs for solvent removal. Finally, generation of waste has to be minimized during product recovery [19,35]. In this respect, it is important to know that MES operates near neutral pH, thus typically producing aqueous carboxylates salts, whereas undissociated hexanoic acid with a purity of >99 % is the target product. It is essential that a recovery method is found that can prevent the stoichiometric formation of a waste sodium salt or another inorganic salt while converting sodium hexanoate to hexanoic acid [32].

Various downstream processing techniques applicable to hexanoic acid, such as solvent extraction, electrodialysis (ED), membrane-assisted recovery, and distillation, have been widely evaluated in conventional bioprocesses [36–43]. ED for instance, is known for achieving high recovery rates; however, it suffers from limited selectivity when separating structurally similar carboxylates, making product-specific recovery challenging [36,37]. For example, one study applied ED with oil-phase recovery to a synthetic MES broth, which resulted in a total carboxylic acid recovery of 60 %. This included hexanoic acid with 76 % purity, although the recovered fraction still consisted of a mixture of various carboxylic acids [38]. In another study, a Polymer Inclusion Membrane (PIM) with ionic liquids extracted hexanoic acid with up to 89 % purity. However, acetic acid was still present [39]. Additionally, previous studies have demonstrated that vapor permeation membrane contactors can achieve over 95 % recovery of carboxylic acids [40], and anion exchange resins have been effectively utilized for organic acid recovery from organic waste [41]. Each of these techniques has its own advantages and disadvantages, depending on the system and target product [32,44,45]. However, these studies did not achieve selective and high-purity separation from mixed carboxylates or demonstrate how hexanoic acid can be purified to over 99 %.

We propose an adsorption/desorption strategy for carboxylate recovery to achieve this goal. Adsorption/desorption using anion exchange resins is a separation technique where negatively charged molecules are first bound to the resin surface (adsorption) and then released with a suitable eluent (desorption). This method is expected to be effective even at low concentrations, as demonstrated in previous work using anion exchange resins for selective C6 and C7 recovery from co-fermented organic waste [34]. In particular, CO_2-expanded methanol enables recovery of carboxylates in their protonated form, prevents the formation of unwanted salt byproducts, and benefits from the high solubility of CO_2 in methanol, which reduces pressure requirements and operating costs [34,46]. Among the available options, this approach is especially promising for MES due to its compatibility with low carboxylate concentrations, high selectivity, and potential to avoid stoichiometric salt waste. Furthermore, using methanol and CO_2 for desorption can minimize waste and facilitate high-purity separation. This makes the method well suited for integration with MES, which uses CO_2 as its primary substrate. This study aims to demonstrate the technical feasibility of integrating MES with this product recovery, highlighting its potential for advancing CO_2 utilization and sustainable chemical production. To this end, we performed lab-scale sorption experiments using simulated MES broth and conducted distillation simulations on an industrial scale. Energy and CO_2 footprint analyses were included to assess the process performance.

2. Materials and methods

2.1. Description of the process configuration

In this initial description of the proposed downstream process, we focus on the desired steady state, knowing that MES has been operated continuously during hundreds of days and that product recovery is preferably performed continuously as well [14]. Fig. 1 shows that the process begins with the utilization of CO_2 and H_2O in the MES (Fig. S1) for biochemical production of carboxylates, while co-producing O_2. At the close to neutral pH required for MES, less than 10 % of the carboxylates is undissociated. During start-up of the MES the Na^+ counterion of the carboxylates is obtained from NaOH used for pH control, but during the steady state that is described here, the neutralization of the produced carboxylic acids and the supply of the Na^+ originates from $NaHCO_3$ in the recycle stream. Due to the biofilm-based nature of the system, more than 99 % of the total biomass remains immobilized, and less than 1 % of microbial cells are suspended in the MES broth [14]. This low biomass content enables efficient separation of carboxylates through low-energy filtration. The filtration step can be performed continuously using a hollow fiber membrane [47] and is required prior to product recovery to remove the residual cells. Part of the carboxylates in the MES outflow is subsequently recovered by adsorption on a column with anion exchange in the bicarbonate form, such that aqueous $NaHCO_3$ is returned to the MES together with non-adsorbed sodium carboxylates. Due to the hydrophobic backbone of the resin, longer carboxylates are expected to bind stronger and to be recovered to a higher extent than shorter carboxylates [34]. When sufficiently loaded with carboxylates, the column is switched to the desorption phase, wherein CO_2-pressurized methanol is introduced to achieve release of the adsorbed carboxylates as uncharged carboxylic acids, since CO_2 can fill the anion-exchange sites with HCO_3^- [34]. The desorbed carboxylic acids in the methanol solution should undergo purification to 99 % through distillation, with some co-production of pure butyric and acetic acids since sorption will not be 100 % selective. Most of the acetate and butyrate, however, should not be adsorbed but should be recycled to MES to serve as hexanoate precursor.

To evaluate the technical feasibility of the proposed process concept, the integrated system was analysed on two different subsystems: (1) MES and adsorption, (2) desorption and distillation.

2.2. Materials

Mixtures containing the main components in the MES were prepared by dissolving acetic acid (≥99 %), butyric acid (≥99 %), hexanoic acid (≥99 %) and $NaHCO_3$ in Milli-Q water (Q-POD® Ultrapure Water Remote Dispenser, MilliporeSigma). NaOH was used to adjust the solution's pH. The solutions used in the experiments are described in Table 1. To accurately observe the differences in behaviour, the concentration of each carboxylic acids was fixed at 1 g L^{-1} in both the carboxylate and carboxylates with bicarbonate conditions, taking into account the column size used in the laboratory setup.

Dowex Marathon MSA, a strong anion exchange resin, was obtained in its chloride form from Sigma Aldrich. The nominal capacity of wet resin was 1.1 eq L^{-1} in Cl^- form. A measured quantity of the wet resin (2.02 g, chloride form, containing 57–62 % *w*/w water) was packed into an Omnifit glass column (1 cm internal diameter × 15 cm height) resulting in a bed volume (BV) of 2.9 mL. Hence, the volume fraction of

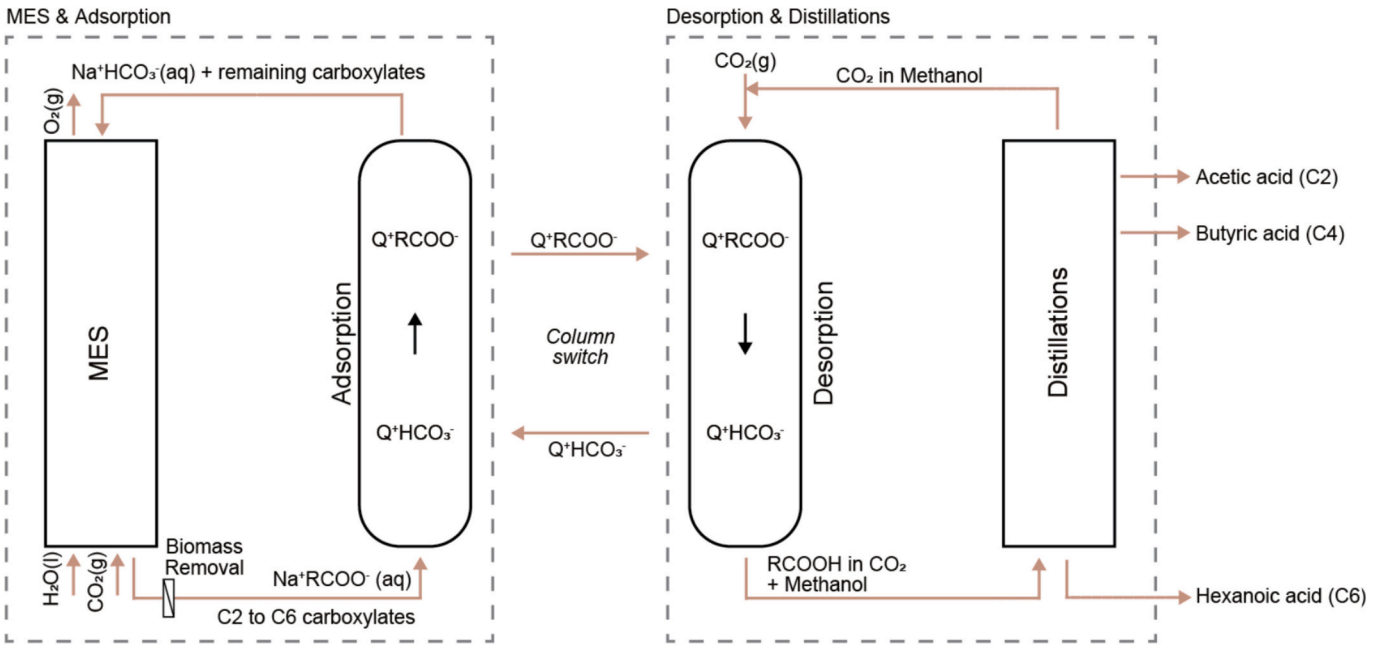

Fig. 1. Conceptual Diagram of the integrated MES, Adsorption/Desorption, and Distillation Process. Q^+ indicates the quaternary ammonium group of the sorbent. R = methyl for C2, propyl for C4 and pentyl for C6.

Table 1
Carboxylate solution compositions.

Aqueous solution name	Acetic acid (g L^{-1})	Butyric acid (g L^{-1})	Hexanoic acid (g L^{-1})	Sodium bicarbonate (g L^{-1})	NaOH (g L^{-1})	pH
Hexanoate	0	0	4	0	1.38	7
	0	0	4	0	1.25	5.8
Carboxylates	1	1	1	0	1.46	7
Carboxylates with bicarbonate	1	1	1	3.69	0.03	7

bulk liquid was estimated at $\varepsilon_L = (2.9–1.9)/2.9 = 0.32$, assuming a water density of 1 g mL^{-1}. Prior to use, the resin was soaked in deionized water overnight, then packed into the column and subsequently converted into its bicarbonate form using a column elution technique [34]. This process involved washing the resin with a continuous flow (1.5 mL min^{-1}) of a sodium bicarbonate solution (20 g L^{-1}) until the conductivity stabilised. Following this step, the resin was rinsed with deionized water at the same flow rate until the conductivity remained unchanged. The column was operated at room temperature. All concentrations in this study are expressed per g wet resin that was initially packed, which contained 0.55 g dry resin per g. To prepare CO_2-expanded methanol, a stainless steel pressure vessel equipped with a pressure gauge and safety relief valve was used. The vessel was sparged with CO_2 from the bottom for 5 min before being filled with methanol to ensure the removal of any residual gas. The vessel was then filled with 100 mL of methanol and pressurized with CO_2 at 10 bar using a mass flow controller [34]. The pressure gauge was monitored to ensure stable operation, and the solvent was used immediately after preparation to avoid pressure loss or degassing. All desorption experiments were performed under controlled pressure conditions to maintain solvent stability.

2.3. Adsorption experiments

A Thermo Scientific Dionex Ultimate 3000 system was used. Carboxylate solutions were pumped through the column at a flowrate of 1.5 mL min^{-1} at room temperature. This corresponds to 0.52 BV (bed volumes) per minute. Fractions of 0.75 mL were collected multiple times throughout the experiment by using a Dionex UltiMate 3000, Automated Fraction collector. Feed and collected samples were stored in refrigerator to analyse carboxylates and pH.

During the experiment, bicarbonate on the anion exchange resin (Q^+) was exchanged with dissociated carboxylates (R_iCOO^-) as shown in Eq. (1).

$$Q^+HCO_3^- + R_iCOO^- \rightleftharpoons Q^+R_iCOO^- + HCO_3^- \quad (1)$$

The breakthrough curve was analysed using C_{out}/C_{feed}, where C_{out} (mM) represents the effluent concentration of the column and C_{feed} (mM) represents its feed concentration. The adsorbed amount in the column Q (mmol g $resin^{-1}$) was calculated using Eq. (2), where F_A (mL min^{-1}) denotes the volume flow rate, t (min) the duration and m (g) represents the wet resin mass.

$$Q = \frac{F_A\left(C_{feed}t - \int_0^t C_{out}dt\right)}{m} \quad (2)$$

The integral in this equation was calculated using data from each sample i:

$$\int_0^t C_{out}dt = \sum_i \left(\frac{C_i + C_{i-1}}{2}\right) \times (t_i - t_{i-1}) \quad (3)$$

The adsorbed amount q (mmol g $resin^{-1}$) was calculated only when equilibration was achieved. This value was obtained by subtracting the amount of solute present in the liquid phase within the column voids from Q. Then, the concentration in bulk liquid at all positions in the column is known to be equal to the feed concentration and was used for subtraction from the amount in the column:

$$q = \frac{F_A\left(C_{feed}t - \int_0^t C_{out}dt\right) - \varepsilon_L \mathrm{BV}\, C_{t,feed}}{m} \quad (4)$$

Selectivity between different carboxylates was calculated at column saturation based on the normalized adsorption per feed concentration, according to the following expression:

$$S_{i/j} = \frac{q_i / C_{i,feed}}{q_j / C_{j,feed}} \quad (5)$$

2.4. Desorption experiments

Desorption experiments were conducted immediately after the adsorption process. To initiate desorption, the solvent in the column was replaced by methanol at a flow rate of 1 mL min^{-1} for 30 min. The CO_2-expanded methanol was subsequently introduced into the column at a flow rate of 1 mL min^{-1}, and 0.75 mL fractions were collected multiple times from the column outlet. These outlet stream was depressurized to atmospheric pressure and connected to the autosampler. Samples were frozen for preservation before analysis. During desorption, the resin was converted back into the bicarbonate form as described in Eq. (6), via a methyl carbonate [46].

$$Q^+R_iCOO^- + H_2O + CO_2 \rightleftharpoons Q^+HCO_3^- + R_iCOOH \quad (6)$$

The concentration factor CF was calculated using Eq. (7), where $C_{i,dmax}$ (mM) represents the maximum concentration of sample after desorption [34].

$$CF = \frac{C_{i,dmax}}{C_{i,feed}} \quad (7)$$

Once no more carboxylates desorbed according to absorbance at 210 nm, the column was rinsed with Milli-Q water at a flow rate of 1 mL min^{-1}, again until constant absorbance.

The desorbed amount in the column N_i (mmol g $resin^{-1}$) was calculated using Eq. (8), where F_D (mL min^{-1}) denotes the volume flow rate of the desorption process. The recovery yield (Y_r, recovery efficiency) of a component was calculated using Eq. (9) [32]. The integral was calculated using Eq. (3).

$$N_i = \frac{F_D\left(\int_0^t C_{D,out}dt\right)}{m} \quad (8)$$

$$Y_r = \frac{N_i}{Q_i} \quad (9)$$

The cumulative desorbed carboxylate ratio (R_i) was calculated using Eq. (10) at each sample i and carboxylate k [48,49].

$$R_i = \frac{\sum_i N_{k,i}}{\sum_k \sum_i N_{k,i}} \quad (10)$$

2.5. Aspen plus simulation and thermodynamic model

The distillation-based purification process was simulated using Aspen Plus software as a computer aided process engineering tool [50]. The NRTL-HOC (Non-Random Two-Liquid with Hayden–O'Connell) property method was employed to accurately represent the phase behaviour of the multicomponent system. This model combines the NRTL activity coefficient model for describing non-ideal interactions in the liquid phase, and the Hayden–O'Connell equation of state, which accounts for vapor-phase association phenomena, particularly the dimerization of carboxylic acids. This thermodynamic framework is well-suited for systems containing methanol, CO_2, and carboxylic acids, enabling reliable estimation of phase equilibria under specific temperature and pressure conditions [50].

2.6. Energy and carbon footprint analysis

The energy consumption and greenhouse gas (GHG) emissions were analysed for the microbial electrosynthesis (MES), adsorption–desorption, and distillation processes (see supplemental information online for calculation details). All values were normalized per kilogram of total recovered carboxylic acids ($kg_{total\ acids}$) and per kilogram of the main product, hexanoic acid ($kg_{hexanoic\ acid}$). Electrical and thermal energy demands were calculated in units of $kW_{el}h$ and $kW_{th}h$, respectively, and converted into CO_2-equivalent emissions (kg CO_{2eq}) using appropriate emission factors for each energy type (Table S2) [50–52].

2.7. Analytical methods

Samples were collected using a HPLC system equipped with an autosampler (DIONEX UltiMate 3000, Thermo Fisher Scientific, USA), during which pH and conductivity were simultaneously measured using a combination pH electrode (Sensorex, USA). Samples (20 µL) were mixed in a polypropylene screw-top vial (Waters, USA) with 200 µL of 1-pentanol solution (320 mg L^{-1}) as internal standard and 200 µL of 1 M H_3PO_4. They were analysed for acetic, butyric, and hexanoic acid concentrations using a Gas Chromatograph (Thermo Fisher, USA) system with a Stabil-wax™ 476 column of 25 m and an internal diameter of 0.2 µm. Helium was used as the carrier gas at a flow rate of 1 mL min^{-1}. The column temperature was kept at 50 °C for 7 min, then increased to 180 °C in 8 min, and kept at that temperature. Flame ionization detection was at 250 °C.

3. Results

3.1. Effect of feed pH on hexanoate adsorption performance

In the proposed process, the carboxylate anion is recovered from the MES broth using an anion exchange resin. Currently, the optimal MES operating condition for maximum productivity is pH 5.8 [14], at which the carboxylates are about 90 % dissociated considering their pK_a values of about 4.8. At pH 7.0, more than 99 % is dissociated (calculated based on the Henderson–Hasselbalch equation). To assess the impact of feed pH, initial adsorption experiments with aqueous hexanoate, the target chemical in this study, were conducted at feed pH 5.8 and 7.0.

The breakthrough curves, column saturation, and pH variations profiles for hexanoate are illustrated in Fig. 2. Column saturation ($C_{out}/C_{feed} = 1$) ends at 27 BV for feed pH 5.8 compared to 99 BV for feed pH 7.0 (Fig. 2A). This indicates that hexanoate adsorption was less at feed pH 5.8, leading to faster resin saturation and quicker allowing hexanoate to pass through. An overshooting phenomenon was observed around 31 BV at pH 5.8, which is likely related to the incomplete dissociation of hexanoic into hexanoate [53]. In contrast, at pH 7.0, the breakthrough curve shows a more gradual increase, suggesting stronger adsorption interactions between fully dissociated hexanoate and the resin [49]. Additionally, at lower pH conditions, bicarbonate is converted to carbonic acid, reducing its competition for adsorption sites. However, the carboxylates also become partially protonated, leading to a lower concentration of their anionic form. This shift in speciation can alter the adsorption equilibrium and influence the overall adsorption behaviour. This enhanced interaction delayed the column saturation and improved hexanoate retention within the column [34]. The column saturation profiles further support these findings, showing that adsorption capacity (Q) at pH 7.0 (1.53 mmol g $resin^{-1}$) is higher and stabilizes at a larger value compared to pH 5.8 (1.00 mmol g $resin^{-1}$) (Fig. 2[B]).

Under feed pH 5.8 conditions, the outflow pH initially exhibits a slight increase before progressively declining and stabilizing around pH 6.0. The initial pH increase is attributed to hexanoate exchange with bicarbonate, in which the released bicarbonate is protonated to a lower extent than hexanoate, because the pK_a values are 4.88 for hexanoic acid

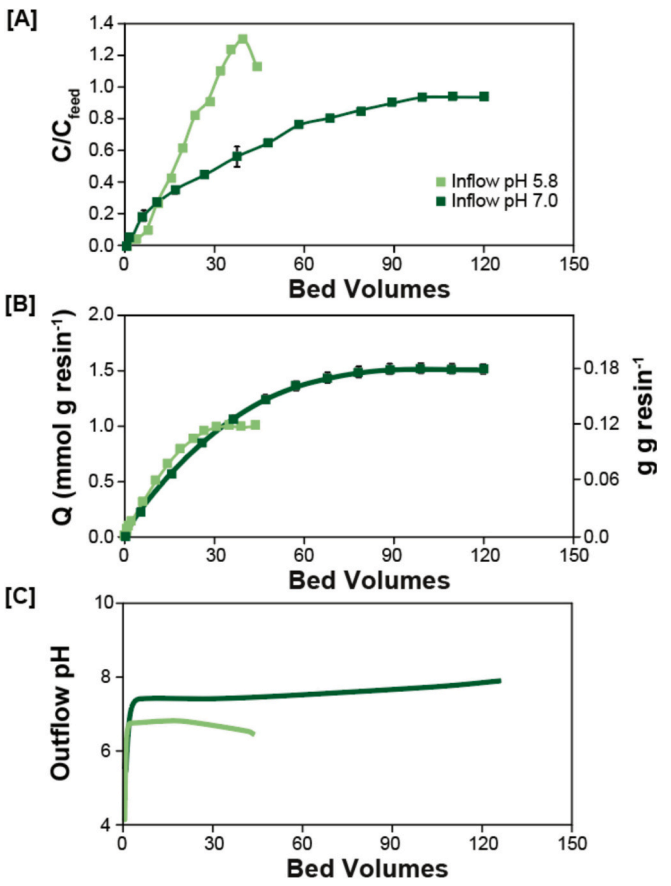

Fig. 2. Column elution with pure aqueous hexanoate at different inflow pH values. [A], Breakthrough curves measured outflow concentration of hexanoate; [B], Calculated loading Q (mmol g resin^{-1}); [C], pH measured at the outflow.

and 6.35 for carbonic acid. Conversely, at pH 7.0, the pH remains stable with a slight upward trend, indicating system stability and suggesting that bicarbonate release or other ion exchange processes had a negligible impact on pH reduction (Fig. 2 [C]). Previous studies have reported that with strong base resins (Amberlyst A26 OH), the adsorption of C2–C4 carboxylates tends to be more favourable in the pH 5–6 range, exhibiting higher adsorption capacities under these conditions [54]. However, our target compound, hexanoate (C6), exhibits greater adsorption amount at pH 7.0. This observation aligns with the breakthrough curve data, confirming enhanced adsorption at pH 7.0 due to stronger interactions between fully dissociated hexanoate and the resin. The loaded column can contain up to 0.17 g hexanoate per g wet resin, indicating that this resin has a sufficiently high capacity for further process development. Therefore, subsequent experiments were conducted while maintaining pH 7.

3.2. *Competitive adsorption behaviour of carboxylates in the presence and absence of bicarbonate*

Carboxylate mixtures with and without containing bicarbonate were compared with respect to adsorption. In all cases, breakthrough was observed at 5.8 BV, with short-chain carboxylates exhibiting faster column saturation (Fig. S2). In the case of the carboxylate mixture (Fig. 3 [A] and [B]), both acetate and butyrate exhibited column saturation at approximately 78 BV, whereas hexanoate displayed the slowest column saturation at 166 BV. At column saturation, hexanoate exhibited the highest accumulation at 0.75 ± 0.01 mmol g resin^{-1}, followed by acetate at 0.54 ± 0.03 mmol g resin^{-1} and butyrate at 0.44 ± 0.01 mmol g resin^{-1}. Notably, acetate exhibited a higher adsorption than butyrate, despite the greater hydrophobicity of butyrate. This discrepancy is attributed to the 47 % higher molar feed concentration of acetate. A previous study using the same resin reported that acetate exhibited greater adsorption than butyrate; however, that study utilized a significantly higher initial acetate concentration (31.6 mM) compared to butyrate (14.1 mM) [31]. The differences were more clearly revealed when comparing selectivity at column saturation. Hexanoate showed the highest selectivity with 2.6 of $S_{Hex/Ac}$ and 2.2 of $S_{Hex/But}$, followed by butyrate (1.2 of $S_{But/Ac}$). The sum of the adsorbed amounts was 1.73 mmol g resin^{-1} (shown in Fig. 3 [B]). This is higher than the 1.52 mmol

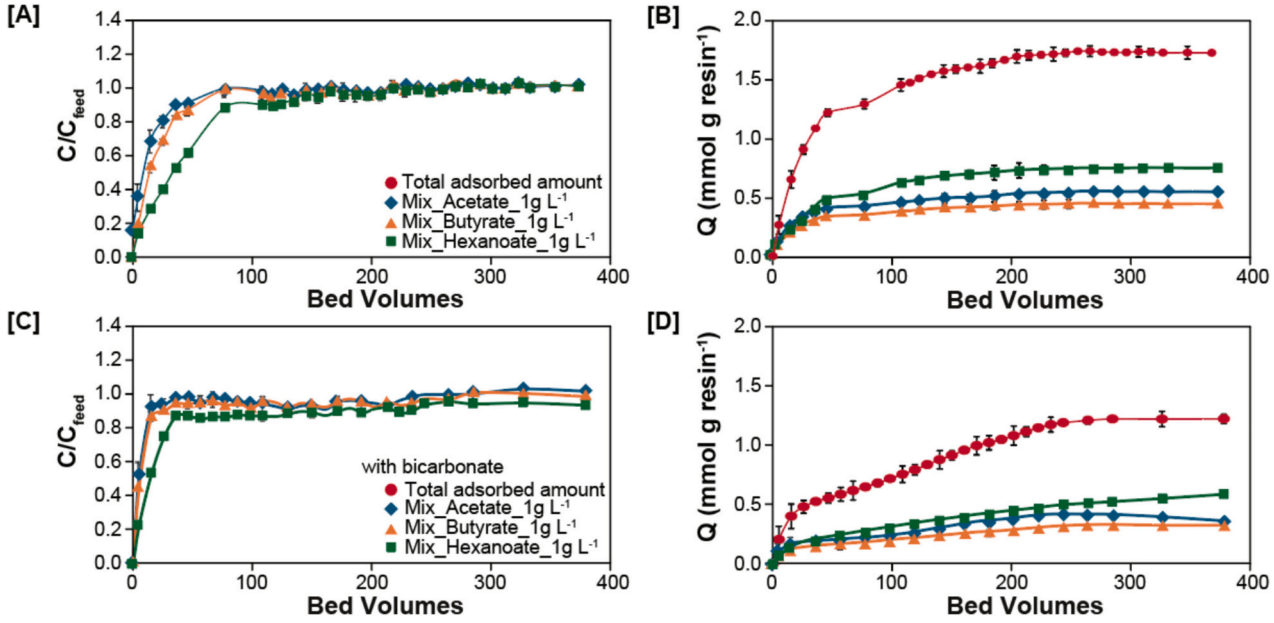

Fig. 3. Breakthrough and column saturation profiles for carboxylate adsorption on an anion-exchange resin. [A] Breakthrough curve for a carboxylate mixture of acetate, butyrate, and hexanoate (1 g L^{-1} each). [B] Column saturation profile for the same mixture. [C] Breakthrough curve for the carboxylate mixture with bicarbonate added (duplicate experiments). [D] Column saturation profile for the mixture with bicarbonate. Feed pH was maintained at 7.0.

g resin^{-1} of Fig. 2 [B]. A similar trend was reported by Liu et al. (2009), where co-adsorption of formic acid and levulinic acid onto 335 resin resulted in a higher total adsorption capacity than either single-component system, suggesting enhanced resin site utilization [55]. Besides carboxylates that pair to the anion exchange sites, there is apparently some binding of sodium carboxylates to the resin backbone and (as multilayer adsorption [56]) to already bound carboxylate. Similar multilayer adsorption phenomena have also been reported for CO_2 and H_2O on quaternary ammonium resins, where hydrogen bonding and ionic interactions facilitate additional binding beyond the primary ion-exchange sites [57]. This will lead to condition-dependent adsorption capacities and selectivities. The significantly higher adsorption capacity of hexanoate in the absence of competing species (1.52 mmol g resin^{-1}; Fig. 2[B]) than under competitive conditions (0.75 mmol g resin^{-1}) highlights the impact of competitive adsorption on overall uptake.

The microbial electrosynthesis (MES) broth contains various growth media components that can negatively impact adsorption amount. Previous adsorption studies using fermentation-derived broths have similarly reported lower adsorption yields in real broth compared to synthetic chemical conditions, mainly due to competitive adsorption among coexisting metabolites and matrix interference [48]. Among the various potential influencing factors (Table S3), bicarbonate was specifically investigated due to its characteristic role in CO_2-reducing MES systems. Since MES continuously supplies CO_2 as a carbon substrate and maintains a pH of 5.8, a high concentration of dissolved CO_2 is expected within the system. However, to mitigate adsorption amount loss, pH is increased (Fig. 2). As a result, due to equilibrium shifts (pK_a: 6.35), dissolved CO_2 is predominantly converted into bicarbonate. To replicate the expected conditions following pH adjustment to 7, the maximum bicarbonate concentration (3.69 g L^{-1}) was estimated based on a simulation study and applied in the experimental validation [58].

The presence of bicarbonate in the feed reduced adsorption across all carboxylates (Fig. 3C and D), with hexanoate, butyrate, and acetate accumulating at 0.67 ± 0.02 mmol g resin^{-1}, 0.32 ± 0.01 mmol g resin^{-1}, and 0.37 ± 0.02 mmol g resin^{-1}, respectively. This corresponds to reductions of 11 %, 27 %, and 33 %, respectively, compared to the carboxylate mixture. These results demonstrate that bicarbonate competes more strongly with acetate and butyrate, leading to a significant reduction in their adsorption. Additionally, the stronger binding affinity of hexanoate promotes its preferential adsorption, further displacing acetate from the resin. To further interpret this trend, literature-reported selectivity values were considered. Prior studies reported selectivity values of $S_{Ac/Cl} = 0.125$ and $S_{HCO_3/Cl} = 0.206$, suggesting that bicarbonate has a higher affinity for the resin than acetate [46]. Using these references, selectivity ratios between carboxylates and bicarbonate were estimated: $S_{Ac/HCO_3} = 0.6$, $S_{But/HCO_3} = 0.7$, and $S_{Hex/HCO_3} = 1.6$. These values support the experimental finding that hexanoate is less affected by bicarbonate due to its stronger binding affinity, which can be attributed to its longer carbon chain that enhances hydrophobic interactions and reduces hydration energy, thereby strengthening its interaction with the resin, allowing it to preferentially adsorb over acetate and butyrate even under competitive conditions [34].

Acetate seemed to reach equilibration at 47 BV, but its concentration kept fluctuating a bit. In contrast, butyrate reached equilibrium at 285 BV, while hexanoate did not reach equilibrium even after 380 BV (Fig. 3 [C]).

In continuous MES operation, bicarbonate levels may fluctuate with gas supply and microbial activity, and our results show that such variations can affect adsorption stability and recovery. Appropriate mitigation or control strategies are needed in large-scale processes, as further discussed in Section 3.6.

3.3. Desorption profile and concentration factor in carboxylate recovery

The desorption profile was evaluated after the adsorption experiments of Fig. 3, so for two conditions: a carboxylate mixture, and a

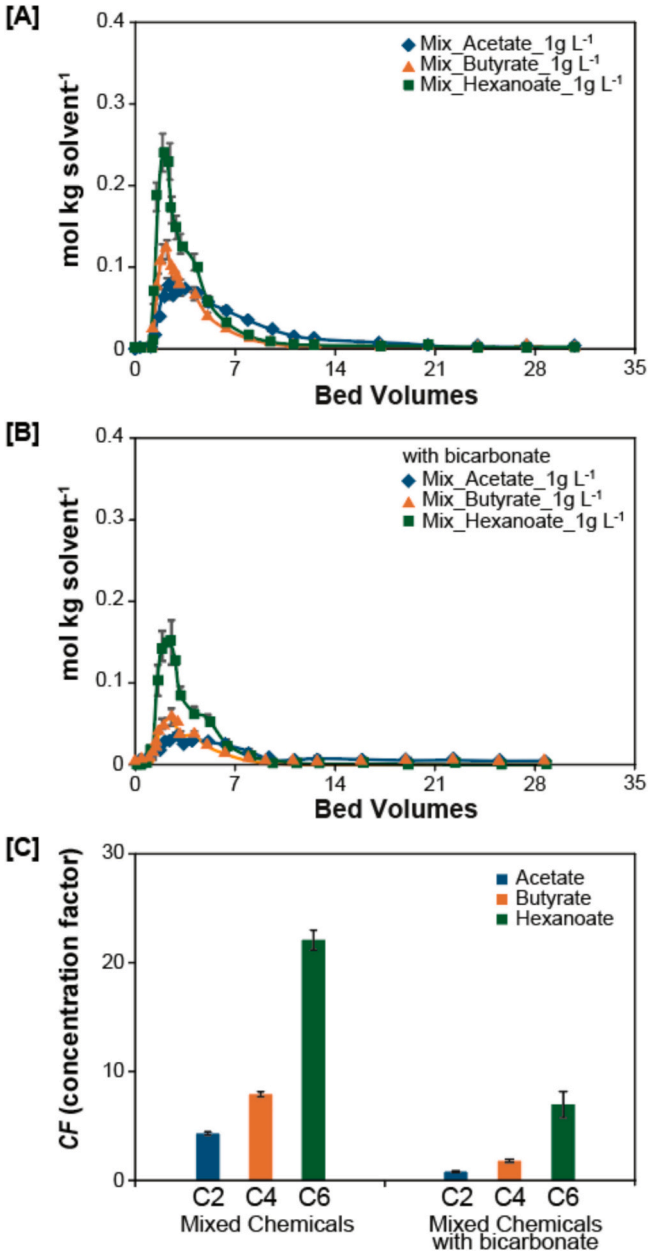

Fig. 4. Desorption performance of carboxylate mixtures using CO_2-expanded methanol. [A] Desorption concentration (in mol kg solvent^{-1}) for the carboxylate mixture and [B] for the carboxylate mixture with bicarbonate, duplicate experiments [C] Concentration factor for the different chemical samples (C2, acetate; C4, butyrate; C6, hexanoate).

Table 2
The adsorbed and desorbed amounts of carboxylates at the end of each process for a carboxylate mixture, and a carboxylate mixture containing bicarbonate at pH 7.

Compound	Carboxylate mixture	Carboxylate mixture with bicarbonate
Adsorbed amount (q,mmol g resin^{-1})		
Acetate	0.54 ± 0.03	0.37 ± 0.02
Butyrate	0.44 ± 0.01	0.32 ± 0.01
Hexanoate	0.75 ± 0.01	0.67 ± 0.02
Desorbed amount in column (*N*,mmol g resin^{-1})		
Acetate	0.58 ± 0.01	0.42 ± 0.03
Butyrate	0.43 ± 0.02	0.25 ± 0.03
Hexanoate	0.77 ± 0.02	0.60 ± 0.02

carboxylate mixture with bicarbonate (Fig. 4 [A] and [B]). The desorbed amounts were close to the adsorbed amounts as shown in Table 2 (Table S4). In Fig. 4[A], where carboxylates mixtures were desorbed, all compounds exhibited a sharp elution peak within the first 2.1 BV, followed by a rapid decline in concentration (Fig. S3). The use of high-pressure CO_2-expanded methanol resulted in a higher initial desorption yield compared to adsorption, facilitating faster extraction from the resin.

These results suggest that early-phase desorption plays a crucial role in maximizing product recovery, highlighting the importance of optimizing the desorption endpoint to prevent loss and ensure high recovery yields. Chandra et al. (2020) reported that in a 2 M NaCl solution, the desorption amount decreased for longer-chain carboxylates due to their increased hydrophobicity, while shorter-chain carboxylates such as formate and acetate exhibited higher adsorption affinities [59]. However, the use of CO_2-expanded methanol facilitated the desorption of all carboxylates. Hexanoate (0.24 ± 0.02 mol kg solvent^{-1}) reached the highest desorption concentration because more hexanoate had been adsorbed than acetate or butyrate. In mixed systems containing bicarbonate, however, competitive interactions between bicarbonate and carboxylates reduced the overall desorbed amounts.

A notable reduction in desorption amount was observed for all carboxylates with bicarbonate present, as shown by the lower concentration peaks (Fig. 4[B]). This is due to bicarbonate competition with carboxylates during adsorption as mentioned before, such that less carboxylate was available for desorption. The impact was particularly significant for hexanoate (0.15 ± 0.03 mol kg solvent^{-1}), which exhibited a substantial decrease in desorption concentration compared to non-bicarbonate conditions. Desorption recovery comparisons further reinforce this finding. Under bicarbonate conditions, however, there was not a close match between adsorbed and desorbed amounts according to Table 2. This discrepancy is likely due to incomplete equilibration during the adsorption stage (Fig. 3[D]), whereas Fig. 3B showed very stable levels at the end of the experiment.

Previous studies have shown that bicarbonate reduces ion exchange by competing with other anions for adsorption sites on the resin, thereby lowering desorption performance and limiting salt removal [60]. Similarly, another study reported a significant decline in anion removal capacity (e.g., Cl^-, NO_3^-) when ammonium bicarbonate was used as the desorption agent [61]. However, in this study, methanol saturated with high-pressure CO_2 was used as the desorption solvent, which likely minimizes the critical limitations associated with bicarbonate.

The bicarbonate concentration tested in this study represents an extreme scenario, as it was calculated based on the pH shift caused by externally supplied CO_2 during MES operation, assuming no microbial CO_2 consumption [58]. However, unutilized CO_2 that remains as dissolved gas after MES leads to bicarbonate at pH 7, causing a significant reduction in adsorbed carboxylate amount and hence to a lower CF during the recovery stage. As shown in Fig. 4 [C], in the mixed carboxylates condition without bicarbonate, the CF for hexanoate reached 22.01 ± 0.9 (C4: 7.9 ± 0.2, C2: 4.3 ± 0.2), whereas under bicarbonate-containing conditions, it dropped to 6.9 ± 1.2 for C6 (C4: 1.8 ± 0.2, C2: 0.7 ± 0.1), representing an approximately 70 % reduction. To address this issue, it is proposed to include a pretreatment step, e.g. mild evaporation, to reduce CO_2 levels before starting the adsorption-desorption process. That step will also increase the feed pH of 5.8 in the direction of pH 7. Hence, the experiments described below are again for a feed at pH 7.0 without bicarbonate.

3.4. Strategic approach to the desorption process for distillation

For practical application in an integrated system, it is essential to establish an optimized desorption strategy because of the trade-off between high recovery yield and high product concentration. For instance, a study evaluated the desorption amount of hexanoic acid using weak anion exchange resins, comparing recovery yield across different solvents [62]. The results showed that a strongly basic resin achieved over 80 % recovery yield. However, the analysis was limited to recovery yield and did not account for the concentration of the recovered product. Another study calculated the concentration factor (CF) at specific desorption points to assess the increase in product concentration compared to the initial feed solution. However, the final concentration of the recovered product was not explicitly considered [34]. In contrast, our study achieved a recovery yield of over 99 % based on the mass amount adsorbed, and also considered the final concentration of the recovered product, thereby presenting a well-balanced desorption strategy that ensures both recovery efficiency and product quality.

As illustrated in Fig. 5A, the desorbed carboxylate ratio varies with bed volume throughout the desorption process. This process was analysed at three distinct points at which desorption might be terminated, to switch back to adsorption: (a), the point where carboxylates were first detected; (b), where the highest pooled concentration (calculated from point (a)) was observed; and (c), where equilibation was complete, as depicted in Fig. 5B and Fig. 5C. Collecting desorption liquid from points (a) to (b) results in a concentrated solution containing hexanoate (13.35 g L^{-1}), butyrate (5.41 g L^{-1}), and acetate (2.77 g L^{-1}), corresponding to recovery yields of 67 %, 64 %, and 35 %, respectively. In contrast, extending desorption to point (c) achieves near-complete recovery (~99 %), but reduces pooled product concentrations to 2.31 g L^{-1} for hexanoate, 0.99 g L^{-1} for butyrate, and 0.92 g L^{-1} for acetate. Additionally, desorption from (b) to (c) results in lower recovery yields of 32 % (hexanoate), 35 % (butyrate), and 65 % (acetate), with product concentrations even lower than those in the initial feed solution. This dilution effect can negatively impact downstream purification, particularly in subsequent distillation processes.

Despite the overall recovery yield at point (b) being 58 % of the total adsorbed carboxylates, the hexanoate concentration is enriched approximately 13-fold compared to the initial feed solution. This suggests that terminating desorption at point (b) is a better compromise between yield and product concentration. However, while point (b) was identified as the best compromise between recovery yield and product concentration, a detailed techno-economic analysis will be required to define the optimal operating window.

Given that a substantial amount of carboxylates remains adsorbed in the column, discarding those upon column regeneration would lead to significant material losses. Therefore, the feasibility of reusing partly desorbed resin columns was investigated. To evaluate reusability, a fresh resin column underwent the same adsorption process, followed by desorption up to point (b) (Fig. 5D). The partly desorbed column was subsequently subjected to another adsorption cycle (Fig. 5E). The adsorption of hexanoate stabilised after approximately 117 BV in both fresh and reused columns (equilibrium at 135 BV), while acetate and butyrate exhibited a marginal increase (~5 %) after 50 BV. These results indicate that the adsorption affinity of C6 is preserved in reused columns, as evidenced by their comparable adsorption profiles. Furthermore, as shown in Fig. 5F, the final adsorption performance of the reused column closely matched that of the fresh column, with only minor differences (1–6 %). Although column reuse does not offer a significant advantage in terms of adsorption kinetics, it enables high-concentration recovery of C6 during desorption.

3.5. Design of multi-stage distillation for high purity carboxylate recovery

Following the desorption process, further distillation steps are necessary to obtain high-purity final products (Fig. 6). After the desorption process at 10 bar, a depressurization step is required to enable atmospheric operation of further distillation steps (further referred to as P2). Lowering the pressure causes CO_2 and some methanol to separate as vapor, which can be achieved using a simple flash unit. This step reduces the total flowrate entering the distillation system (by ~4.4 %), allowing for smaller equipment units downstream. Moreover, it increases the concentration of valuable acids in the liquid phase,

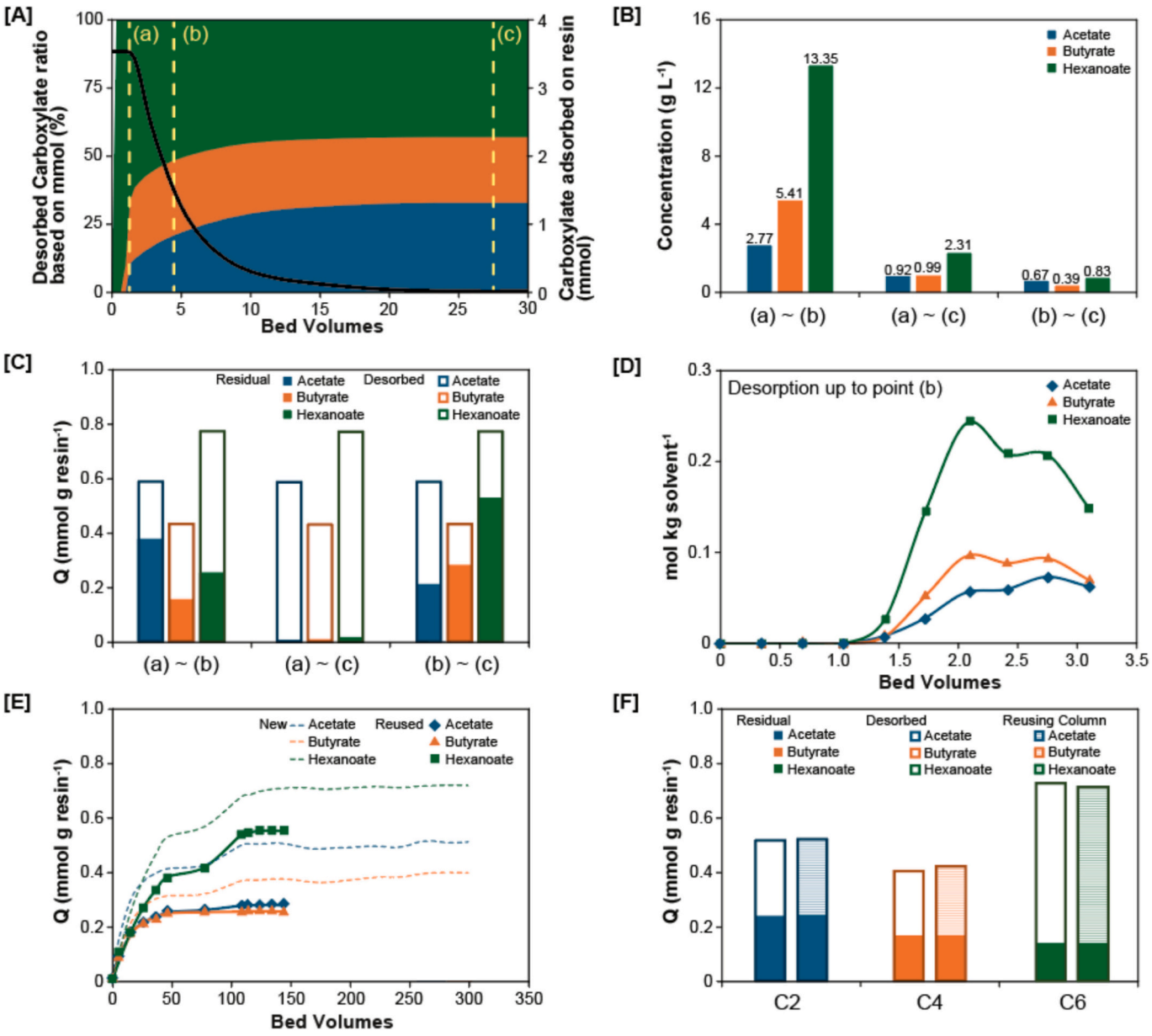

Fig. 5. [A] Desorbed carboxylate ratio during the desorption process (coloured areas) and residual carboxylates (black line) in the resin, where (a) 1.38 BV, (b) 4.48 BV, and (c) 27.59 BV. [B] Cumulative carboxylate concentration in the collected samples between (a)–(b), (a)–(c), and (b)–(c). [C] Comparison of residual adsorbed and desorbed amounts between (a)–(b), (a)–(c), and (b)–(c). [D] The column with fresh resin was operated in the adsorption process with a carboxylate mixture, followed by the desorption process, which was carried out up to point (b). [E] Comparison of new and reused column saturation for the carboxylate mixture. [F] The residual adsorbed and desorbed amounts in the new and reused columns for carboxylate mixture saturation (hatched box).

thereby reducing the overall distillation energy requirements.

After the initial vapor separation, the remaining liquid stream is sent to the first distillation column (COL1) to separate most of the remaining CO_2 and methanol. Due to the presence of CO_2, a partial vapor-liquid condenser is necessary for this column. In principle, a partial condenser operates by cooling the overhead vapor stream to a set temperature at which part of the condensable vapor condenses while the non-condensable gases remain in the vapor phase. This allows effective separation, since the condensed liquid can be returned as reflux or withdrawn as distillate, while the non-condensable gases can be vented or treated separately. By doing so, the condenser helps to maintain stable column operation and prevent the accumulation of non-condensable gases. Proper selection of the distillate vapor fraction should allow the usage of inexpensive cooling utilities for the condenser of this column. Nonetheless, this separation is highly energy intensive as it requires evaporation of more than 90 wt% of the feed. Therefore, minimizing reboiler duty for column COL1 may be crucial for reducing the overall energy consumption of the process. Theoretically, the remaining CO_2 and methanol can be completely separated in the vapor and liquid distillates [63]. In this case, the mixture of acetic, butyric and hexanoic acids would be obtained in the bottom product. However, this would lead to a large temperature difference between the top and the bottom stages of the distillation column (>100 °C), which complicates the application of heat pumps. Alternatively, adjusting a distillate-to-feed ratio in this column may allow separation of all CO_2 with most of the methanol in the vapor and liquid distillates, as the ratio controls the distribution of volatile (CO_2) and less volatile (methanol) components within the column, while ensuring sufficiently close boiling points of the top and bottom products for application of mechanical vapor recompression (MVR). This heat pump system implies compressing vapor from

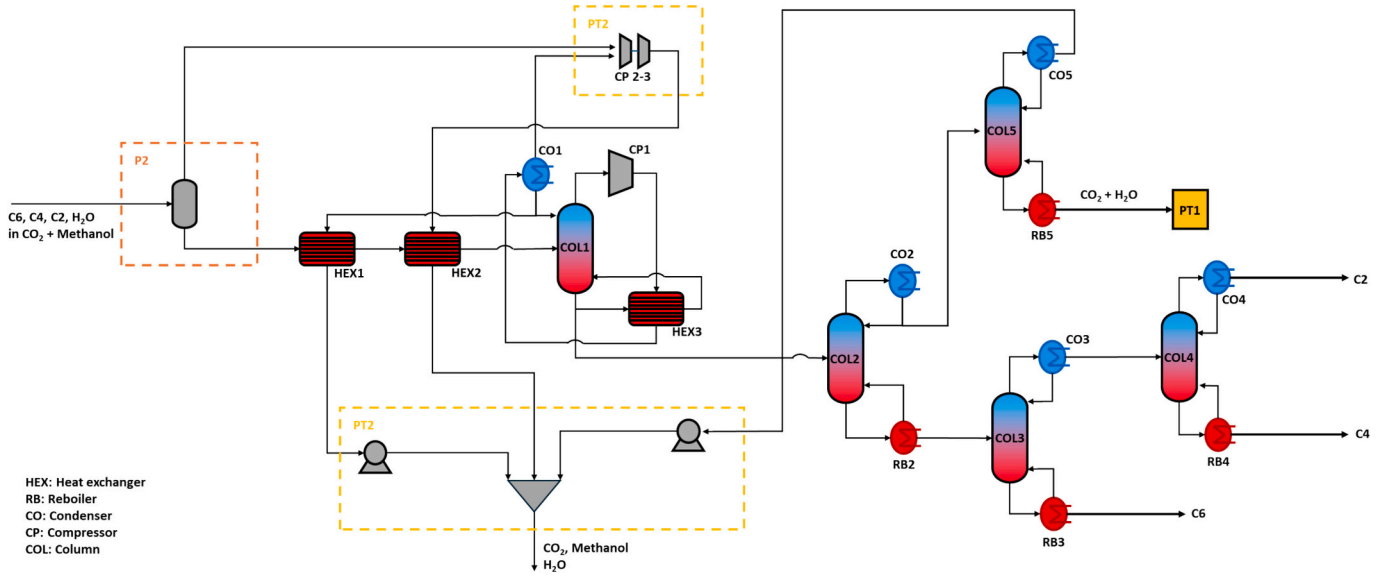

Fig. 6. Schematic of the distillation process including flash separation, multi-stage distillation (COL1–COL5), and MVR-assisted heat integration. Abbreviations: HEX, heat exchanger; RB, reboiler; CO, condenser; CP, compressor; COL, column; P2, pretreatment; PT2, post-treatment.

the top of a distillation column and using it instead of a heating utility in the reboiler of the distillation column. Hence, electrical energy, required to power the compressor, may replace significantly higher thermal energy requirements [52]. Moreover, the scalability of this concept has already been demonstrated in industrial applications such as bioethanol and organic acid distillation [64,65]. Besides reducing overall energy requirements, this heat pump system may enable complete (green) electrification of this step.

Furthermore, additional heat integration is possible to reduce the reboiler duty of distillation column COL1, which further reduces the required compressor power in the MVR system. More precisely, reduction in the reboiler duty of COL1 decreases the heat demand at the column bottom, so the overhead vapor requires less compression to supply sufficient reboiler heat, thereby lowering the compressor power in the MVR system. The vapor and liquid distillates from this column, composed of CO_2 and methanol, can be reused in the desorption process. However, liquid distillate needs to be cooled before being recycled. This cooling requirement presents an opportunity to recover heat by using liquid distillate to preheat the subcooled feed entering column COL1. Likewise, the vapor distillate must be compressed to 10 bar before it can be reused (further referred to as PT2). As a result of compression, its temperature increases, and additional cooling becomes necessary. This hot vapor stream can also serve as a heat source for preheating the feed to column COL1.

Following the separation in column COL1, an additional distillation step is required to separate the remaining methanol from the carboxylic acids. This may be performed in the second distillation column (column COL2). High-purity methanol is recovered as a top product and can be reused in the desorption step. The bottom product, containing a mixture of carboxylic acids, is directed to further purification steps.

In the next distillation column (column COL3), high purity hexanoic acid (>99.7 wt%) can be separated as the bottom product, while a mixture of acetic and butyric acid is obtained at the top. There are two potential options for handling this overhead stream: it can either be recycled back to the microbial electrosynthesis (MES) process for further chain elongation, or it can be fed to a fourth distillation column (column COL4) designed to separate high-purity acetic acid and butyric acid as the top and bottom products, respectively.

In case water is used to wash the adsorption/desorption columns, small amounts of water may be present in the feed stream to the distillation part of the purification process. Most of this water would be separated with methanol in the distillate of column COL2. Additionally, some water may also be present in the liquid distillate of column COL1. If recycling this water to the desorption is unfavourable, it may be separated from the distillate of column COL2 in an additional distillation step (fifth distillation column COL5). Specifically, COL5 separates residual water from the COL2 distillate to ensure high-purity methanol for reuse, thereby protecting microbial activity and supporting closed-loop solvent recycling. However, separating small amounts of water from the liquid distillate from column COL1 is not recommended as evaporating methanol from this stream would be very energy intensive.

3.6. *Proposing integrated process for MES, adsorption-desorption, and distillation*

Based on the measured and simulated data in this study, a process integrating MES, adsorption-desorption, and distillation is proposed, as illustrated in Fig. 7. Assuming that C2, C4, and C6 compounds are each produced at a concentration of 1 g L^{-1} in MES, the proposed process suggests that the fermentation broth first undergoes a pre-treatment step (P1) before entering the adsorption column. In P1, the first step involves a filtration process to remove residual microbial cells from the MES broth. The second step is the removal of dissolved CO_2, which primarily exists in the gas phase at pH 5.8; this CO_2 can either be vented externally or recirculated as a feed gas into the MES reactor. Venting CO_2 already leads to a pH increase, which reduces the need for base addition. Finally, the pH is adjusted to 7 (in this study) to stabilise the solution before it proceeds to the adsorption column.

During the adsorption step, when the column is operated at 135 BV, which corresponds to the breakthrough point for C6, the adsorption yield for C6, C4, and C2 are 36 %, 15 %, and 14 %, respectively. The lower adsorption yield as compared to Section 3.3 is due to the reuse of columns, as demonstrated in Section 3.4. Under these conditions, 64 % of C6 is recirculated, reducing the inhibitory effect of C6 accumulation on microbial growth. Additionally, 86 % of C2 and 85 % of C4 are recirculated, providing sufficient precursors for chain elongation and subsequent C6 production. Before reinjecting the stream into the MES reactor, a post-treatment step (PT1) is required. This step involves the recirculation of both the stream recovered after adsorption and the CO_2 driven water from distillation. However, instead of undergoing separate physical or chemical treatments, it is more appropriate to adjust the recycling rate based on the operating conditions of MES and circulate

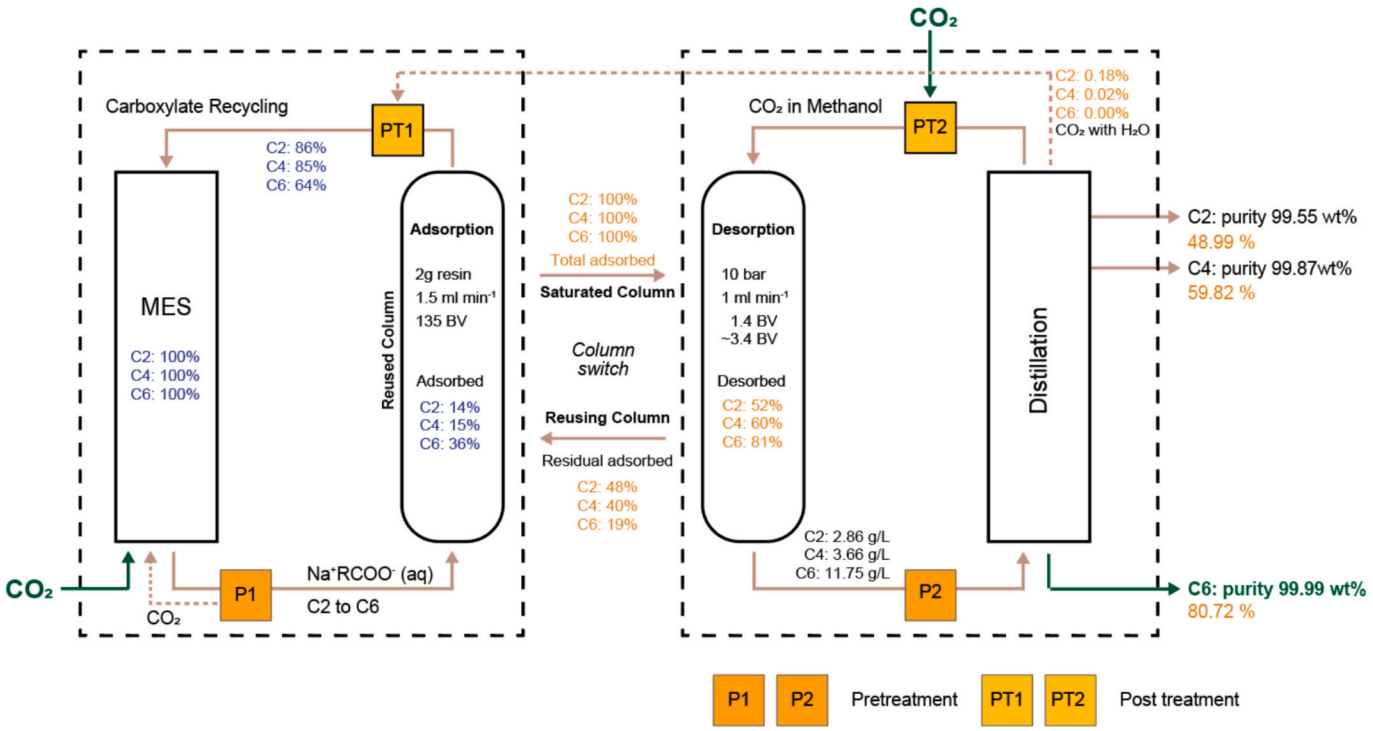

Fig. 7. Integrated process diagram including MES, Adsorption, Desorption, and Distillation processes. Pretreatment (P1 and P2) and post-treatment (PT1 and PT2) were proposed to complete the full process.

the stream accordingly. Ideally, if the composition and concentration of the medium supplied to MES is controlled within PT1, the stream could be fully reused for MES. In addition, after the adsorption process, the solution stabilizes at pH 7.8–8.0 and utilizing this stream can minimize the need for additional pH adjustments in conventional MES operations. Therefore, integrating this process helps maintain overall pH balance while offsetting the base addition costs in P1.

After column switching, the desorption step releases 81 % of the adsorbed C6, 60 % of C4, and 52 % of C2. The initial 1.4 BV of methanol is sent to the distillation that recovers solvent, to remove residual impurities, as carboxylate concentrations are nearly zero in this fraction. The desorption process is conducted between 1.4 BV and 3.4 BV, after which a fraction of carboxylates remains bound to the resin. The resulting concentrations of the recovered compounds are C6 at 11.75 g L^{-1}, C4 at 3.66 g L^{-1}, and C2 at 2.86 g L^{-1}, indicating that C6 has been concentrated over 11-fold compared to its initial concentration. Although this value is lower than the C6 concentration in Fig. 5B (13.35 g L^{-1}), this discrepancy is attributed to column pressure conditions and the inability to immediately remove methanol in the present setup, leading to some losses. In the current lab-scale experimental setup, a pressure control valve is installed between the column and the sampler (outlet) to regulate pressure. When the sample is collected, it passes through this valve before reaching the sampler, where the pressure is reduced to atmospheric pressure. Due to these conditions, if the desorption process is stopped, additional desorption reactions and chemical losses occur within the column and the valve-to-sampler line as a result of the pressure drop. This partial loss explains the lower observed concentration. Further optimization of immediate pressure reduction systems and desorption stop timing is expected to lead to higher concentrations. Moreover, in conventional desorption processes, a basic solution is typically used to release carboxylates, followed by the addition of an acid to convert them back into hexanoic acid, requiring an additional acid treatment step. However, by utilizing CO_2-expanded methanol, it is possible to recover hexanoic acid directly during desorption without the need for this additional neutralization step.

In the proposed integrated process, P2 is applied prior to distillation to release dissolved CO_2 and a portion of methanol under high pressure, thereby reducing the system pressure. This step decreases the liquid flow rate entering the distillation system and increases the concentration of valuable acids in the liquid phase, thereby reducing energy consumption in the subsequent distillation. During P2, over 40 % of CO_2 along with some methanol is separated in the vapor phase. This stream is sent to the purification stage in the distillation columns, where the products are separated. Finally, high-purity hexanoic acid (>99 wt%) is obtained as the final product, along with pure acetic acid (>99 wt%) and butyric acid (>99 wt%). A small amount of residual CO_2 and water is directed to the PT1 process, while the majority of the separated CO_2 and methanol is recycled to the desorption process via the PT2 step.

Ultimately, the proposed integrated process establishes a fully closed-loop system with no material waste, enabling the complete internal recycling of key process streams. Through the effective coupling of MES, adsorption–desorption, and distillation, this system not only maximizes resource utilization but also achieves the selective and high-purity recovery of hexanoic acid directly from CO_2. Moreover, the process is expected to be scalable and operate reliably given its basis in commercially established unit operations. In the following section, we further evaluate the feasibility of this integrated system from the perspectives of energy consumption and CO_2 footprint.

3.7. Energy and carbon footprint analysis

To evaluate the integrated process proposed in this study, we calculated the energy consumption and carbon emissions associated with each step. The calculated integrated process is schematically illustrated in Fig. 8. For accurate analysis, electrical and thermal energy demands were separately quantified across the entire process. To ensure practical relevance, CO_2 equivalents were calculated based on grey electricity for electrical energy and natural gas as the source for thermal energy.

In the MES section, the external electrical energy (W_{el}) required for microbial production was 19.3 $kW_{el}h\ kg_{total\ acids}^{-1}$, while 2.0 $kW_{th}h\ kg_{total\ acids}^{-1}$ of thermal energy (W_{th}) was required to maintain the reactor

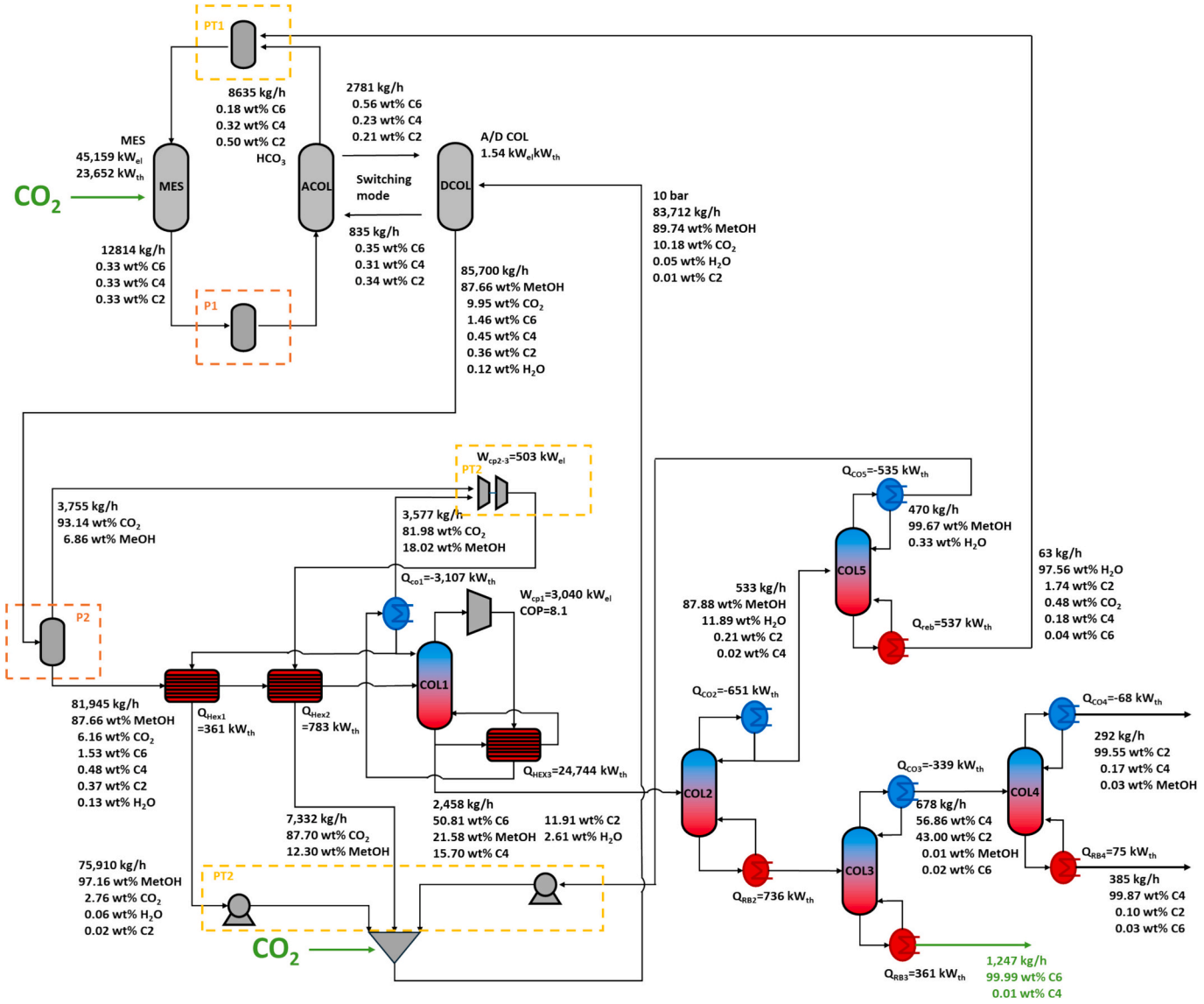

Fig. 8. Integrated process diagram of MES, adsorption/desorption, and distillation units, including estimated energy consumption and product recovery pathways.

temperature. The total energy requirements of MES are 20.1 $kW_{el}h$ $kg^{-1}_{total\ acids}$ (equivalent to 50.3 $kW_{th}h$ $kg^{-1}_{total\ acid}$). This value is relatively high compared to previous reports [31], which is mainly due to the intentionally low productivity set in this study (1 g L^{-1} for each of C2, C4, and C6 chemicals). The adsorption and desorption processes operate at ambient temperature, meaning the only energy required is for circulating the MES broth. The energy demand for this circulation was 0.8 $W_{el}h$ $kg^{-1}_{total\ acids}$, which is negligible compared to other stages. Since methanol and CO_2 used in desorption are mostly recycled (after the initial phase) and merged into the distillation system (P2 and PT2), their energy demand is included in the distillation stage.

The final separation by distillation may be highly energy-intensive, primarily due to the large quantities of methanol that must be evaporated (>12 $kW_{th}h$ $kg^{-1}_{total\ acids}$). However, the implementation of the previously described MVR heat pump system can significantly reduce overall energy demand. The coefficient of performance (COP), defined as the ratio of exchanged heat to required compressor power, of this system is approximately 8.1. For reference, COP values above 2.5 (a conservative benchmark for electrical-to-thermal conversion) indicate high energy conversion yield [52], confirming the effectiveness of the proposed heat pump integration.

The vapor separated in step P2, along with the liquid and vapor distillates from column COL1, can be effectively recycled within the system, improving overall resource utilization. Nevertheless, to maintain optimal desorption conditions, these streams must be pressurized to 10 bar and may be used to preheat the feed entering column COL1. This heat integration strategy may reduce the reboiler duty of COL1 by approximately 4.4 %.

Subsequent distillation steps, namely in columns COL2, COL3, COL4 and COL5, are significantly less energy-intensive, with their combined reboiler duties accounting for less than 7 % of that of COL1. Ultimately, approximately 4.80 $kW_{th}h/kg_{total\ acids}$ (including 0.85 $kW_{th}h/kg_{total\ acids}$ for thermal energy and 1.58 $kW_{el}h/kg_{total\ acids}$ for electricity) are required to recover high-purity hexanoic acid (>99.7 wt%) and a mixture of butyric and acetic acids that can recycled into MES for further chain elongation. Alternatively, to recover both butyric acid (>99.8 wt %) and acetic acid (>99.6 wt%) in high purity, an additional 0.04 $kW_{th}h/kg_{total\ acids}$ is needed, bringing the total to 4.84 $kW_{th}h/kg_{total\ acids}$. Accounting for the energy requirements in PT2 (compression and pumping to 10 bar), total energy requirements of P2, distillation and PT2 steps are 5.49 $kW_{th}h/kg_{total\ acids}$ (equivalent to 2.20 $kW_{el}h/kg_{total\ acids}$ and 8.47 $kW_{th}h/kg_{hexanoic\ acid}$). In both scenarios, implementing advanced heat pumping (mechanical vapor recompression) and heat integration techniques, plays a critical role in lowering process energy

requirements. These strategies have the potential to reduce overall energy demand by approximately 66 %.

A previous report proposed an integrated MES and liquid–liquid extraction process targeting 99 % purity hexanoic acid, with an energy requirement of 31.04 kWh $kg^{-1}_{total\ acids}$ [19]. However, this analysis relied on optimistic assumptions, including a faradaic efficiency (FE) of 100 % and 80 % of the converted carbon directed towards C6), and did not account for the stoichiometric generation of waste salts. In contrast, our study reports a more realistic energy requirement (22.29 $kW_{el}h\ kg_{total\ acids}^{-1}$, 99 % purity) based on experimentally observed values (FE of 88 % and only 33 % carbon recovery as C6). Despite employing more realistic operating conditions, the overall process exhibited lower energy requirements.

Another study reported the production of MCCA oil with a purity of over 72 % at a specific energy consumption as low as 6.2 kWh kg^{-1}_{oil} using a pertraction and membrane electrolysis process [66]. While this process demonstrated low energy input, the product purity was substantially lower. Notably, when considering only the product recovery stage in the present study, 99 % purity hexanoic acid was obtained at 2.2 $kW_{el}h\ kg^{-1}_{total\ acids}$.

Collectively, these results demonstrate that the process developed herein is highly applicable for real-world implementation. Furthermore, In the overall integrated process, the MES stage accounts for 91 % of the total energy demand, with 87 % of the entire energy input corresponding to electricity required for MES (Fig. 9 [A]). This indicates that most of the energy consumed in the integrated system is directly supplied as electrons to support microbial production. It is also worth noting that the current energy demand was calculated based on a conservative MES productivity; thus, further improvements in productivity would likely result in a substantial reduction in energy consumption per unit of product. In the MES process, CO_2 is the sole carbon source, and 1.94 kg $CO_{2eq}\ kg^{-1}_{total\ acids}$ is consumed. Meanwhile, under the assumption of using grey electricity, the entire integrated system emits 9.91 kg $CO_{2eq}\ kg^{-1}_{total\ acids}$ (Fig. 9 [B]). When expressed per mass of the main product, hexanoic acid, the MES stage contributes 13.82 kg $CO_{2eq}\ kg^{-1}_{hexanoic\ acid}$, while downstream processes add 1.44 kg $CO_{2eq}\ kg^{-1}_{hexanoic\ acid}$, resulting in a total emission of 15.27 $CO_{2eq}\ kg^{-1}_{hexanoic\ acid}$. The system offsets approximately 19.6 % of its gross emissions by directly incorporating CO_2 into the product. Compared to previous work, which reported 2.25 $CO_{2eq}\ kg^{-1}_{hexanoic\ acid}$ for product recovery based on liquid–liquid extraction [19], the current process achieves 36 % lower emissions for the downstream processing steps. Notably, our proposed system not only recovers hexanoic acid at >99.9 % purity but also enables the recovery of acetic and butyric acids at >99 % purity. Moreover, all methanol and CO_2 used in the desorption are fully recycled within the system. In the proposed integrated process, the largest contributor to carbon emissions is the electricity required to power the MES stage. If MES efficiency is improved to reduce electricity demand, and green electricity is used across the entire integrated process, carbon-negative operation becomes a realistic possibility. Assuming the use of green electricity (50 % solar, 50 % wind) [67], the overall CO_2 emission is reduced to 0.75 $CO_{2eq}\ kg^{-1}_{total\ acids}$ suggesting that the system can potentially operate in a carbon-negative manner within our gate-to-gate context (Fig. 9 [B]). Nevertheless, integrating renewable electricity into the proposed concept remains a practical challenge, requiring consideration of intermittency, storage, and grid integration, which should be addressed in future work.

4. Conclusion

This study developed an integrated microbial electrosynthesis (MES), adsorption–desorption, and distillation process for the high-yield and resource-conscious recovery of C6 carboxylic acid from CO_2 conversion. The adsorption step selectively captured 36 % of C6, while 86 % of C2 and 85 % of C4 were recirculated to support further chain elongation. CO_2-expanded methanol enabled efficient desorption, releasing

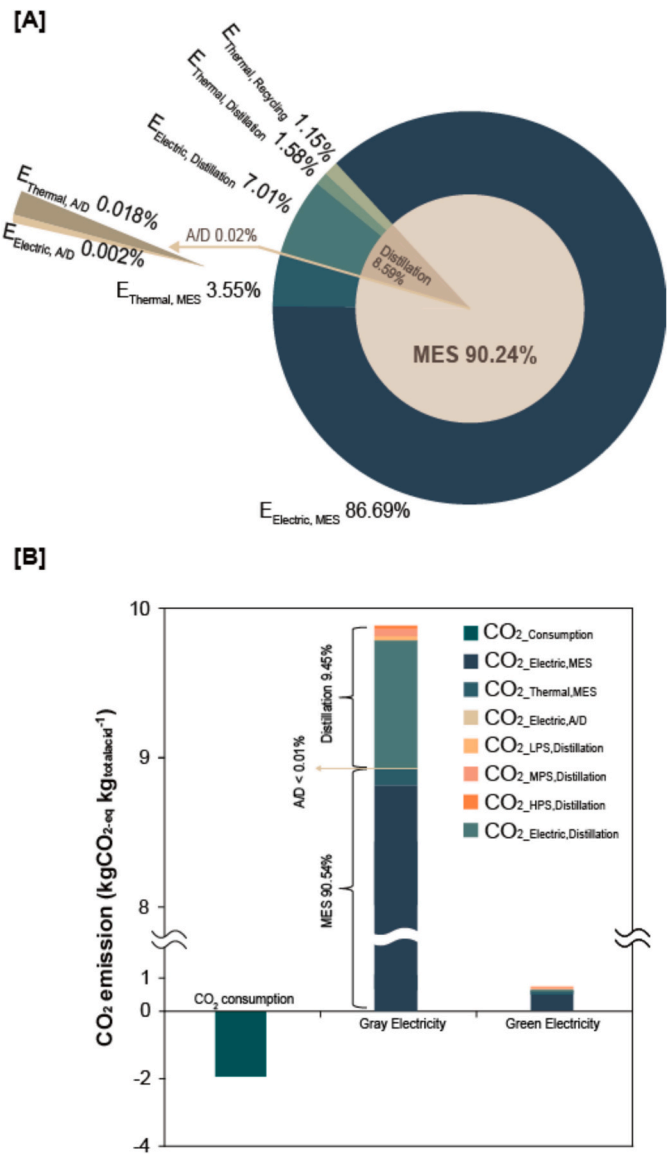

Fig. 9. [A] Proportion of energy demand by process in the integrated system, and [B] CO_2 consumption and CO_2 emissions.

81 % of the adsorbed C6, with methanol and CO_2 fully recycled within the system. Distillation-based final purification further allowed the recovery of high-purity hexanoic acid (>99.9 wt%), while butyric and acetic acids could either be recycled as a mixture or recovered individually at >99.6 wt% purity. Incorporating pretreatment (bicarbonate removal and CO_2 release) and post-treatment steps (pH stabilization, water, methanol, and CO_2 recycling) reduced energy demand and improved resource utilization. The total calculated energy requirement was 55.72 kWthh kg total $acids^{-1}$, of which 87 % originated from the external electron supply in the MES step. When powered by green electricity, total emissions decreased to 0.75 kg CO_2eq kg total $acids^{-1}$, lower than the 1.96 kg CO_2eq kg total $acids^{-1}$ fixed in MES, indicating the potential for carbon-negative operation. Taken together, these findings suggest that the proposed design represents one of the most sustainable MES product recovery processes reported to date, and future studies should further evaluate its long-term stability, techno-economic and life-cycle feasibility as essential prerequisites for scale-up.

CRediT authorship contribution statement

Mungyu Lee: Writing – review & editing, Writing – original draft, Visualization, Validation, Supervision, Investigation, Formal analysis, Data curation, Conceptualization. **Tamara Jankovic:** Visualization, Software. **Francisco Caparrós-Salvador:** Data curation, Conceptualization. **Ludovic Jourdin:** Writing – review & editing, Supervision, Funding acquisition, Conceptualization. **Adrie J.J. Straathof:** Writing – review & editing, Supervision, Funding acquisition, Conceptualization.

Declaration of competing interest

The authors declare that they have no known competing financial interests or personal relationships that could have appeared to influence the work reported in this paper.

Acknowledgements

This project received funding from the project “C1to6: CO2 into hexanoic acid using microbial electrosynthesis” (NWO OTP 19771).

Appendix A. Supplementary data

Supplementary data to this article can be found online at https://doi.org/10.1016/j.cej.2025.169412.

Data availability

Data will be made available on request.

References

[1] S.Y. Leong, S.R.M. Kutty, P.Y. Moh, Q. Li, Upcycling of carbon from waste via bioconversion into biofuel and feed, in: Carbon Dioxide Capture and Conversion, 2022, pp. 65–92.
[2] C. Zhang, R. Fu, L. Kang, Y. Ma, D. Fan, Q. Fei, An upcycling bioprocess for sustainable aviation fuel production from food waste-derived greenhouse gases: life cycle assessment and techno-economic analysis, Chem. Eng. J. 486 (2024) 150242.
[3] S. Overa, B.H. Ko, Y. Zhao, F. Jiao, Electrochemical approaches for CO2 conversion to chemicals: a journey toward practical applications, Acc. Chem. Res. 55 (5) (2022) 638–648.
[4] C. Karakaya, J. Parks II, Thermochemical processes for CO2 hydrogenation to fuels and chemicals: challenges and opportunities, Appl. Energy Combust. Sci. 15 (2023) 100171.
[5] G.H. Han, J. Bang, G. Park, S. Choe, Y.J. Jang, H.W. Jang, S.Y. Kim, S.H. Ahn, Recent advances in electrochemical, photochemical, and photoelectrochemical reduction of CO2 to C2+ products, Small 19 (16) (2023) 2205765.
[6] Y. Wang, S. Cheng, C. Varrone, Z. Liu, Z. He, A. Zhou, X. Yue, A. Wang, W. Liu, Selective colonization of multifunctional microbes that facilitates caproate production in microbial electrosynthesis system, Chem. Eng. J. 488 (2024) 150848.
[7] D. Suri, L.M. Aeshala, T. Palai, Microbial electrosynthesis of valuable chemicals from the reduction of CO2: a review, Environ. Sci. Pollut. Res. 31 (25) (2024) 36591–36614.
[8] H. Su Kim, S. Lee, M. Moon, H. Jong Jung, J. Lee, Y.H. Chu, J. Rae Kim, D. Kim, G. Woo Park, C. Hyun Ko, Enhancing microbial CO2 electrocatalysis for multicarbon reduction in a wet amine-based catholyte, ChemSusChem 17 (11) (2024) e202301342.
[9] L. Jourdin, T. Burdyny, Microbial electrosynthesis: where do we go from here? Trends Biotechnol. 39 (4) (2021) 359–369.
[10] T. Zheng, C. Xia, Electrifying biosynthesis for CO2 upcycling, Trends Chem. 5 (1) (2023) 7–10.
[11] M. Ravichandran, T.T.A. Kumar, R. Dineshkumar, Carbon dioxide capture, sequestration, and utilization models for carbon management and transformation, Environ. Sci. Pollut. Res. 31 (44) (2024) 55895–55916.
[12] M.A. Zegers, E. Augustijn, G. Jongbloed, L. Jourdin, Novel miniaturised microbial electrosynthesis reactor: a study on replicability, Chem. Eng. J. 163881 (2025).
[13] E. Blanchet, F. Duquenne, Y. Rafrafi, L. Etcheverry, B. Erable, A. Bergel, Importance of the hydrogen route in up-scaling electrosynthesis for microbial CO 2 reduction, Energ. Environ. Sci. 8 (12) (2015) 3731–3744.
[14] O. Cabau-Peinado, M. Winkelhorst, R. Stroek, R. de Kat Angelino, A.J.J. Straathof, K. Masania, J.M. Daran, L. Jourdin, Microbial electrosynthesis from CO2 reaches productivity of syngas and chain elongation fermentations, Trends Biotechnol. 42 (11) (2024) 1503–1522.
[15] W.-T. Ren, Z.-L. He, Y. Lv, H.-Z. Wang, L. Deng, S.-S. Ye, J.-S. Du, Q.-L. Wu, W.-Q. Guo, Carbon chain elongation characterizations of electrode-biofilm microbes in electro-fermentation, Water Res. 267 (2024) 122417.
[16] K. Zhang, Y. Chen, T. Song, X.L. Li, J. Xie, Simultaneous utilization of glucose and xylose from biomass facilitate the chain elongation of microbial electrosynthesis, J. Environ. Chem. Eng. 13 (5) (2025) 117600.
[17] X. Ji, L. Huang, Z. Chen, R. Chen, J. Zhu, Hexanoic acid production from anaerobic fermentation of Chinese cabbage waste with exogenous lactic acid as electron donor, J. Environ. Chem. Eng. 12 (6) (2024) 114518.
[18] S. Agnihotri, D.-M. Yin, A. Mahboubi, T. Sapmaz, S. Varjani, W. Qiao, D. Y. Koseoglu-Imer, M.J. Taherzadeh, A glimpse of the world of volatile fatty acids production and application: a review, Bioengineered 13 (1) (2022) 1249–1275.
[19] J. Luo, M. Pérez-Fortes, A.J.J. Straathof, A. Ramirez, Life cycle assessment of hexanoic acid production via microbial electrosynthesis and renewable electricity: future opportunities, J. Environ. Chem. Eng. 12 (5) (2024) 113924.
[20] E.C. Canapi, Y.T. Agustin, E.A. Moro, E. Pedrosa Jr., M.L.J. Bendaño, Coconut oil, in: Bailey’s industrial oil and fat products, 2005.
[21] K. Rajesh, M. Natarajan, P. Devan, S. Ponnuvel, Coconut fatty acid distillate as novel feedstock for biodiesel production and its characterization as a fuel for diesel engine, Renew. Energy 164 (2021) 1424–1435.
[22] M. Roy, M. Saich, S.A. Patil, Scalability of the microbial electro-acetogenesis process for biogas upgradation: performance and technoeconomic assessment of a liter-scale system, Energy Fuel 37 (20) (2023) 15822–15831.
[23] M. Roy, R. Yadav, P. Chiranjeevi, S.A. Patil, Direct utilization of industrial carbon dioxide with low impurities for acetate production via microbial electrosynthesis, Bioresour. Technol. 320 (2021) 124289.
[24] S. Li, M. Kim, Y.E. Song, S.H. Son, H.-i. Kim, J. Jae, Q. Yan, Q. Fei, J.R. Kim, Housing of electrosynthetic biofilms using a roll-up carbon veil electrode increases CO2 conversion and faradaic efficiency in microbial electrosynthesis cells, Bioresour. Technol. 393 (2024) 130157.
[25] M.T. Noori, Mansi, S. Sundriyal, V. Shrivastav, B.S. Giri, M. Holdynski, W. Nogala, U.K. Tiwari, B. Gupta, B. Min, Copper foam supported g-C3N4-metal–organic framework bacteria biohybrid cathode catalyst for CO2 reduction in microbial electrosynthesis, Sci. Rep. 13 (1) (2023) 22741.
[26] J. Luo, M. Pérez-Fortes, P. Ibarra-Gonzalez, A.J.J. Straathof, A. Ramirez, Impact of intermittent electricity supply on a conceptual process design for microbial conversion of CO2 into hexanoic acid, Chem. Eng. Res. Des. 205 (2024) 364–375.
[27] T. Zhang, H. Nie, T.S. Bain, H. Lu, M. Cui, O.L. Snoeyenbos-West, A.E. Franks, K. P. Nevin, T.P. Russell, D.R. Lovley, Improved cathode materials for microbial electrosynthesis, Energ. Environ. Sci. 6 (1) (2013) 217–224.
[28] L.P. Thulluru, M.M. Ghangrekar, S. Chowdhury, Progress and perspectives on microbial electrosynthesis for valorisation of CO2 into value-added products, J. Environ. Manage. 332 (2023) 117323.
[29] J.C. Wood, J. Grové, E. Marcellin, J.K. Heffernan, S. Hu, Z. Yuan, B. Virdis, Strategies to improve viability of a circular carbon bioeconomy-A techno-economic review of microbial electrosynthesis and gas fermentation, Water Res. 201 (2021) 117306.
[30] P.O. Saboe, L.P. Manker, W.E. Michener, D.J. Peterson, D.G. Brandner, S.P. Deutch, M. Kumar, R.M. Cywar, G.T. Beckham, E.M. Karp, In situ recovery of bio-based carboxylic acids, Green Chem. 20 (8) (2018) 1791–1804.
[31] L. Jourdin, J. Sousa, N. van Stralen, D.P. Strik, Techno-economic assessment of microbial electrosynthesis from CO2 and/or organics: an interdisciplinary roadmap towards future research and application, Appl. Energy 279 (2020) 115775.
[32] C.S. López-Garzón, A.J.J. Straathof, Recovery of carboxylic acids produced by fermentation, Biotechnol. Adv. 32 (5) (2014) 873–904.
[33] P. Dessì, L. Rovira-Alsina, C. Sánchez, G.K. Dinesh, W. Tong, P. Chatterjee, M. Tedesco, P. Farràs, H.M. Hamelers, S. Puig, Microbial electrosynthesis: towards sustainable biorefineries for production of green chemicals from CO2 emissions, Biotechnol. Adv. 46 (2021) 107675.
[34] C. Fernando-Foncillas, C.I. Cabrera-Rodríguez, F. Caparrós-Salvador, C. Varrone, A. J.J. Straathof, Highly selective recovery of medium chain carboxylates from co-fermented organic wastes using anion exchange with carbon dioxide expanded methanol desorption, Bioresour. Technol. 319 (2021) 124178.
[35] M. Quraishi, K. Wani, S. Pandit, P.K. Gupta, A.K. Rai, D. Lahiri, D.A. Jadhav, R. R. Ray, S.P. Jung, V.K. Thakur, Valorisation of CO2 into value-added products via microbial electrosynthesis (MES) and electro-fermentation technology, Fermentation 7 (4) (2021) 291.
[36] M. Lee, J.-H. Kim, M. Yasin, S.-H. Moon, I.S. Chang, A sustainable bioprocessing system leveraging gas fermentation and bipolar membrane electrodialysis system for direct recovery of acetic acid, Chem. Eng. J. 490 (2024) 151710.
[37] J.-H. Kim, M. Lee, H. Jeong, S. Ko, S.-H. Moon, I.S. Chang, Recycling of minerals with acetate separation in biological syngas fermentation with an electrodialysis system, Chem. Eng. J. 459 (2023) 141555.
[38] P.A. Hernandez, M. Zhou, I. Vassilev, S. Freguia, Y. Zhang, J.r. Keller, P. Ledezma, B. Virdis, Selective extraction of medium-chain carboxylic acids by electrodialysis and phase separation, ACS Omega 6 (11) (2021) 7841–7850.
[39] B.-Y. Wang, N. Zhang, Z.-Y. Li, Q.-L. Lang, B.-H. Yan, Y. Liu, Y. Zhang, Selective separation of acetic and hexanoic acids across polymer inclusion membrane with ionic liquids as carrier, Int. J. Mol. Sci. 20 (16) (2019) 3915.
[40] S. Aydin, H. Yesil, A.E. Tugtas, Recovery of mixed volatile fatty acids from anaerobically fermented organic wastes by vapor permeation membrane contactors, Bioresour. Technol. 250 (2018) 548–555.
[41] S. Rebecchi, D. Pinelli, L. Bertin, F. Zama, F. Fava, D. Frascari, Volatile fatty acids recovery from the effluent of an acidogenic digestion process fed with grape pomace by adsorption on ion exchange resins, Chem. Eng. J. 306 (2016) 629–639.
[42] J. Kang, S.H. Kim, Y.K. Hwang, B.T.D. Nguyen, J. Kim, J.F. Kim, Scalable membrane-assisted ion exchange (MEM-IE) strategy for organic acid purification in biorefinery process, J. Membr. Sci. 715 (2025) 123442.

[43] H. Wu, T. Kim, S. Ferdous, T. Scheve, Y. Lin, L. Valentino, M. Holtzapple, T. R. Hawkins, P.T. Benavides, M. Urgun-Demirtas, Sustainable aviation fuel from high-strength wastewater via membrane-assisted volatile fatty acid production: experimental evaluation, techno-economic, and life-cycle analyses, ACS Sustain. Chem. Eng. 12 (18) (2024) 6990–7000.
[44] A.G. Santos, T.L. de Albuquerque, B.D. Ribeiro, M.A.Z. Coelho, In situ product recovery techniques aiming to obtain biotechnological products: a glance to current knowledge, Biotechnol. Appl. Biochem. 68 (5) (2021) 1044–1057.
[45] W. Zhao, V. Jegatheesan, Q. Liang, K. Soontarapa, H. Jiang, Y. Zhang, B. Yan, Towards high carbon conversion efficiency by using a tailored electrodialysis process for in-situ carboxylic acids recovery, J. Clean. Prod. 297 (2021) 126431.
[46] C.I. Cabrera-Rodríguez, C.M. Cartin-Caballero, E. Platarou, F.A. de Weerd, L.A. van der Wielen, A.J.J. Straathof, Recovery of acetate by anion exchange with consecutive CO2-expanded methanol desorption: a model-based approach, Sep. Purif. Technol. 203 (2018) 56–65.
[47] M. Lee, M. Yasin, N. Jang, I.S. Chang, A simultaneous gas feeding and cell-recycled reaction (SGCR) system to achieve biomass boosting and high acetate titer in microbial carbon monoxide fermentation, Bioresour. Technol. 298 (2020) 122549.
[48] F. Raganati, A. Procentese, G. Olivieri, M.E. Russo, P. Salatino, A. Marzocchella, Bio-butanol separation by adsorption on various materials: assessment of isotherms and effects of other ABE-fermentation compounds, Sep. Purif. Technol. 191 (2018) 328–339.
[49] E. Morselli, S. Notarfrancesco, G.A. Martinez, J.M. Domingos, A. Negroni, M. Mancini, F. Fava, L. Bertin, Recovery of carboxylic acids from actual effluent by using sequential cationic-anionic adsorption steps at semi pilot scale, J. Environ. Chem. Eng. 12 (5) (2024) 114089.
[50] I. Aspen Technology, Aspen Plus | Leading Process Simulation Software, 2025.
[51] B.P. Flannery, J.W. Mares, The Greenhouse Gas Index for Products in 39 Industrial Sectors, Working paper., Resources for the Future, Washington, DC, 2022.
[52] A.A. Kiss, C.A.I. Ferreira, Heat Pumps in Chemical Process Industry, CRC Press, 2016.
[53] C. Kassar, C. Graham, T.H. Boyer, Removal of perfluoroalkyl acids and common drinking water contaminants by weak-base anion exchange resins: impacts of solution pH and resin properties, Water Res. X 17 (2022) 100159.
[54] C. Fargues, R. Lewandowski, M.-L. Lameloise, Evaluation of ion-exchange and adsorbent resins for the detoxification of beet distillery effluents, Ind. Eng. Chem. Res. 49 (19) (2010) 9248–9257.
[55] B.-J. Liu, Z.-J. Hu, Q.-L. Ren, Single-component and competitive adsorption of levulinic/formic acids on basic polymeric adsorbents, Colloids Surf. A Physicochem. Eng. Asp. 339 (1–3) (2009) 185–191.
[56] Y.-C. Wu, Y.-H. Wei, H.-S. Wu, Adsorption and desorption behavior of ectoine using Dowex® HCR-S ion-exchange resin, Processes 9 (11) (2021) 2068.
[57] G.N. Tomaraei, S. Binney, R. Stratton, H. Zhuang, J.L. Wade, H2O and CO2 Sorption in Ion Exchange Sorbents: Distinct Interactions in Amine Versus Quaternary Ammonium Materials, arXiv preprint arXiv:2508.03909, 2025.
[58] O. Cabau-Peinado, A.J.J. Straathof, L. Jourdin, A general model for biofilm-driven microbial electrosynthesis of carboxylates from CO2, Front. Microbiol. 12 (2021) 669218.
[59] A. Chandra, S. Chattopadhyay, Chain length and acidity of carboxylic acids influencing adsorption/desorption mechanism and kinetics over anion exchange membrane, Colloids Surf. A Physicochem. Eng. Asp. 589 (2020) 124395.
[60] Y. Hu, J. Foster, T.H. Boyer, Selectivity of bicarbonate-form anion exchange for drinking water contaminants: influence of resin properties, Sep. Purif. Technol. 163 (2016) 128–139.
[61] C.I. Cabrera-Rodríguez, M. Moreno-González, F.A. de Weerd, V. Viswanathan, L. A. van der Wielen, A.J.J. Straathof, Esters production via carboxylates from anaerobic paper mill wastewater treatment, Bioresour. Technol. 237 (2017) 186–192.
[62] R. Singh, S. Palar, A. Kowalczewski, C. Swope, P. Parameswaran, N. Sun, Adsorptive recovery of volatile fatty acids from wastewater fermentation broth, J. Environ. Chem. Eng. 11 (5) (2023) 110507.
[63] J.H. Yoon, H.S. Lee, H. Lee, High-pressure vapor-liquid equilibria for carbon dioxide+ methanol, carbon dioxide+ ethanol, and carbon dioxide+ methanol+ ethanol, J. Chem. Eng. Data 38 (1) (1993) 53–55.
[64] A.L. Rispoli, G. Rispoli, N. Verdone, A. Salladini, E. Agostini, M. Boccacci, M. P. Parisi, B. Mazzarotta, G. Vilardi, The electrification of conventional industrial processes: the use of mechanical vapor compression in an EtOH–water distillation tower, Energies 14 (21) (2021) 7267.
[65] R.T.C.R.a. PILLER, Mechanical Vapor Recompression in Whisky Production: Chivas Brothers Case Study, 2024.
[66] J.M. Carvajal-Arroyo, S.J. Andersen, R. Ganigué, R.A. Rozendal, L.T. Angenent, K. Rabaey, Production and extraction of medium chain carboxylic acids at a semi-pilot scale, Chem. Eng. J. 416 (2021) 127886.
[67] W.B. Moomaw, P., G. Heath, M. Lenzen, J. Nyboer, A. Verbruggen, IPCC special report on renewable energy sources and climate change mitigation, annex II: methodology, in: O.P.-M. Edenhofer, R., Y. Sokona, K. Seyboth, P. Matschoss, S. Kadner, T. Zwickel, P. Eickemeier, G. Hansen, S. Schlömer, C. von Stechow (Eds.), Intergovernmental Panel on Climate Change (IPCC), Cambridge, United Kingdom and New York, NY, USA, 2011, pp. 975–1000.